Carbohydrate Polymers 83 (2011) 545–553

Contents lists available at ScienceDirect

Carbohydrate Polymers

journal homepage: www.elsevier.com/locate/carbpol

Characterization and functional elucidation of a fucosylated 1,6-α-D-mannogalactan polysaccharide from *Antrodia cinnamomea*

Jing-Jy Cheng [1], Mei-Kuang Lu [1], Cha-Yui Lin, Chia-Chuan Chang *

National Research Institute of Chinese Medicine, 155-1 Li-Nung St., Sec. 2, Shipai, Peitou, Taipei 112, Taiwan

ARTICLE INFO

Article history:
Received 14 July 2010
Received in revised form 4 August 2010
Accepted 9 August 2010
Available online 17 August 2010

Keywords:
Antrodia cinnamomea
Polysaccharide
Mannogalactan
Angiogenesis
Angiopoietin-2
VEGFR

ABSTRACT

Antrodia cinnamomea is a valuable polyporaceous edible fungus native to Taiwan. It was reported to provide a number of pharmaceutical benefits. *A. cinnamomea* was cultured, the polysaccharides (PSs) were extracted and chromatographically fractionated, and their biological functions were evaluated. The PS subfractions (B85PS-I–V) showed differential inhibition of *in vitro* Matrigel tube formation (an indicator of angiogenesis inhibition) with IC_{50} values of 7.44, 16.41, 7.07, 7.98, and 16.33 μg/ml, respectively. Furthermore, *A. cinnamomea* PSs also blocked vascular endothelial growth factor (VEGF)-induced endothelial cell migration. B85PS-III and -V dose-dependently decreased angiogenic-related protein expressions, including inhibition of VEGF receptor (VEGFR) phosphorylation and angiopoietin-2 protein expression. To further purify and determine the structure of the bioactive PS, B85PS-III was chromatographically purified to give a water-soluble partial fucosylated 1,6-α-D-mannogalactan (B85PS-III-1) composed of a nonadecasaccharide repeating unit with a molecular mass of 4.17×10^2 kDa as shown below. The chemical structure of B85PS-III-1 was characterized by a monosaccharide analysis along with ^1H, ^{13}C, and 2D nuclear magnetic resonance spectroscopy.

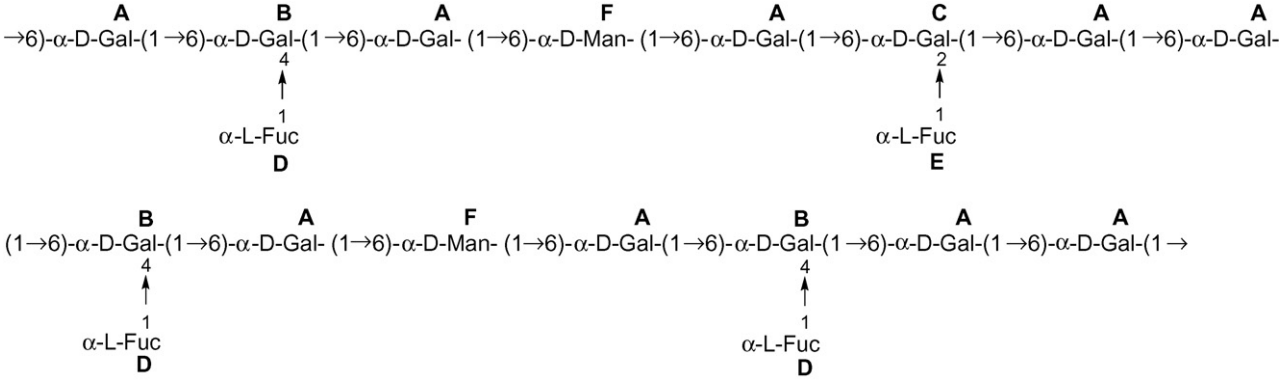

1. Introduction

Antrodia cinnamomea (*niu-chang-chih* in Chinese) is a valuable medicinal and edible fungus of the family Polyporaceae that only grows on the brown heartwood of *Cinnamomum kanehirae* Hayata (stout camphor tree, Lauraceae) (Wu, Ryvarden, & Chang, 1997) in Taiwan. Recent research revealed numerous pharmaceutical benefits of *A. cinnamomea*, including hepatoprotective (Hsu et al., 2005), immunomodulative (Cheng, Hsu, Chen, & Lee, 2008; Lu et al., 2009), antiviral (Lee et al., 2002), anticancer (Chang et al., 2008), anti-inflammatory (Shen et al., 2004), and antioxidative (Huang & Mau, 2007) activities. Chemical components found in *A. cinnamomea* include phenolics (Chiang, Wu, Cherng, & Ueng, 1995), diterpenoinds, steroids, lignans (Wu & Chiang, 1995), triterpenes (Cherng, Wu, & Chiang, 1996), maleic acid derivatives, and polysaccharides (PSs) (Lee et al., 2002).

* Corresponding author. Tel.: +886 2 28201999x6641; fax: +886 2 28264266.
E-mail address: changch@nricm.edu.tw (C.-C. Chang).
[1] These two authors contributed equally to this work.

0144-8617/$ – see front matter © 2010 Elsevier Ltd. All rights reserved.
doi:10.1016/j.carbpol.2010.08.016

The PSs of *A. cinnamomea* demonstrate antiangiogenic (Liu et al., 2004; Yang, Zhou, Wang, & Hu, 2009) and immunomodulatory effects (Chen et al., 2008; Cheng, Hsu, et al., 2008). In a previous paper, we reported the chemical composition and anti-inflammatory effect of a lipopolysaccharide (LPS) from *A. cinnamomea* with totally different bioactivities from bacteria (Cheng, Yang, Cheng, Wang, Huang, & Lu, 2005), and a PS from liquid culture of *A. cinnamomea* that inhibited cyclin D1 expression by inhibiting vascular endothelial growth factor receptor (VEGFR) signaling, leading to the suppression of angiogenesis (Cheng, Huang, Chang, Wang, & Lu, 2005). We herein reported the purification, characterization, and antiangiogenic effect of a novel high-galactose-type PS from an *in vitro* culture system of *A. cinnamomea*. Angiogenesis is responsible for tumor development in early stages and is rate limiting for tumor progression (Karamysheva, 2008). Vascular endothelial growth factor (VEGF) and angiopoietin-2 (Ang-2) play crucial roles in balancing tumor growth and vascular regression (Hanahan, 1997). Ang-2 is a secreted factor, the expression of which is upregulated at sites of angiogenesis. VEGF, bovine fetal growth factor (bFGF), and hypoxia are shown to induce the expression of Ang-2 in bovine microvascular endothelial cells (ECs), thus contributing to a deterioration in the integrity of preexisting vasculature (Mandriota & Pepper, 1998). Therefore, antiangiogenic components are now considered to be good candidates for cancer therapy (Boehm, Folkman, Browder, & O'Reilly, 1997).

In this study, we attempted to determine the structure of bioactive PSs extracted from *A. cinnamomea*. A novel PS (denoted B85PS-III-1) composed of a 1,6-α-D-mannogalactosyl main skeleton with partial α-L-fucosyl terminals was reported.

2. Materials and methods

2.1. Fermentation of A. cinnamomea B85

PSs were isolated from 10-day-old fermentation of *A. cinnamomea* (Lu, Cheng, Lai, Lin, & Huang, 2008).

2.2. Isolation and purification of PSs

Isolation and purification of PS were carried out according to Lu's method (Lu, Cheng, Lin, & Chang, 2010). After being dissolved in the aforementioned buffer, 40 mg of the PS was fractionated into fractions I–V (see Fig. 1A).

2.3. Homogeneity and molecular weight

B85PS-III (4.8 mg) was purified by high-performance size exclusion chromatography (SEC) with an RI detector (Viscotek model 301) equipped with two SEC columns (G4000PW$_{XL}$ 7.8 mm × 300 mm and G3000PW$_{XL}$ 7.8 mm × 300 mm, Viscotek) into 1–3 fractions (Fig. 1B). The flow rate was 0.5 ml/min, with deionized water as the eluent. Purified fraction 1 (denoted B85PS-III-1, 1.7 mg) was used for the following structural determination. A PS solution in Milli-Q water was diluted to give a concentration of 1 mg/ml. The sample injection volume was 0.1 ml. The molecular weight of B85PS-III-1 was determined by the same system. A calibration curve was constructed using a series of standards, Sodex P-82 series (Showa Denko, Mentor, OH) containing polymaltotriose with molecular weights of 788, 404, 212, 112, 47.3, 22.8, 11.8, and 5.9 kilodaltons (kDa).

2.4. Monosaccharide analysis

Sugar composition of PS was determined after acid hydrolysis of PSs, and carried out according to Cheng's method (Cheng, Lin, Lur, Chen, & Lu, 2008).

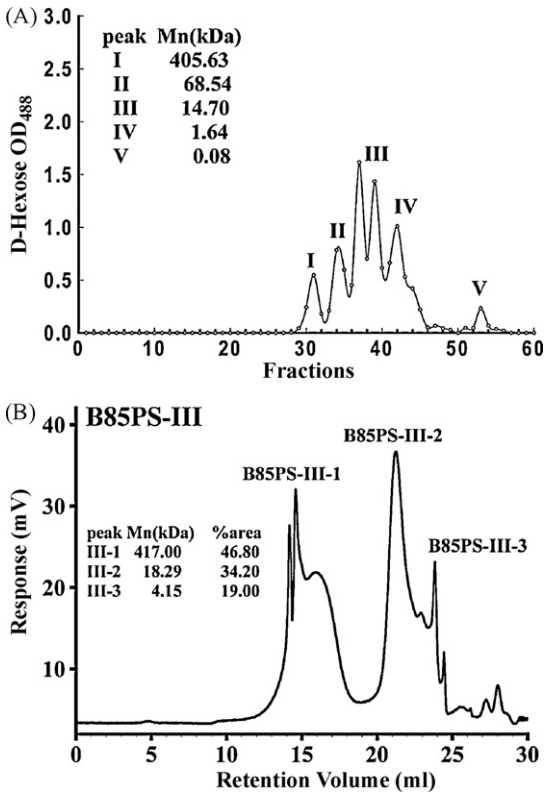

Fig. 1. Fractionation and purification of polysaccharides (PSs) of *Antrodia cinnamomea*. (A) Fractionation of PSs by gel filtration column chromatography into Fr-I (28–32), -II (33–36), -III (37–40), -IV (41–50), and -V (51–56); (B) size-exclusion chromatography (SEC) of fraction III (AC-B85-III) using G4000PW$_{XL}$ and G3000PW$_{XL}$ (Viscotek) columns (fraction 1: 24.0–37.3 ml; fraction 2: 37.3–45.3 ml; fraction 3: 45.3–52.4 ml).

2.5. EC culture

Endothelial cells were cultured as previous described (Cheng, Lin, et al., 2008). In brief, ECs were cultured in Dulbecco's modified Eagle's medium (DMEM) (Life Technologies, Paisley, UK) supplemented with 10% heat-inactivated fetal bovine serum (FBS) (Life Technologies).

2.6. Matrigel EC tube formation assays

Matrigel tube formation was performed as previously described (Cheng, Lin, et al., 2008). In brief, Matrigel was applied onto a 96-well plate and allowed to solidify, then ECs were seeded. After adhesion of the cells, the medium was removed and replaced by fresh medium supplemented (or not) with tested PSs and incubated at 37 °C for 18 h. The tubes of growth were visualized with an inverted Nikon/TMS microscope at a magnification of 4×, and the length of the capillary network was quantified with a map scale calculator (KURABO Angiogenesis Image Analysis Software).

2.7. Wound healing assay

Endothelial cell migration was determined by means of a wound healing migration assay using a commercial product, Culture-Insert (iBidi GmbH, Germany). A scratch of 0.5 mm in width was made according to the manufacturer's manual. ECs were treated with or without tested PS 1 h before VEGF. The cells that had migrated across the edge of the wound were photographed under a microscope. A fixed width with no migrated cell was obtained as control group, then migrated cells numbers were calculated of each group in the same width to present migration ability.

2.8. Immunoblotting

ECs were lysed with buffer containing 0.1% sodium dodecylsulfate (SDS) and 2-mercaptoethanol, and then subjected to SDS-polyacrylamide gel electrophoresis (PAGE). Proteins were identified with identical monoclonal antibodies. Antigen–antibody complexes were detected using horseradish peroxidase (HRP)-labeled rabbit anti-mouse immunoglobulin G (IgG), and results were analyzed using an enhanced chemiluminescence (ECL) system (Pierce, Rockford, IL). The blots were exposed to Kodak XAR-5 film (Rochester, NY) to obtain the fluorographic images.

2.9. 1D and 2D NMR

The lyophilized sample of B85PS-III-1 (1.7 mg) was dissolved in 0.5 ml of D_2O (99.9%, Cambridge Isotope Laboratories, Andover, MA). The 1D and 2D NMR spectra of B85PS-III-1 were acquired by a Varian VNMRS NMR spectrometer (600 MHz) at 25 °C and a Varian 5-mm Cold Probe. The reference chemical shifts for ^1H and ^{13}C NMR were calibrated to δ_H 4.78 (HDO) and δ_C 30.89 (acetone-d_6, which was added as an internal reference), respectively. 2D ^1H–^1H correlation spectra were obtained by the standard pulse sequence of double-quantum filter-correlated spectroscopy (DQF-COSY). The TOCSY spectrum was obtained using a 100 ms mixing time and 2 s relaxation delay. The NOESY (nuclear overhauser effect spectroscopy) and HSQC (heteronuclear single quantum coherence) spectra were obtained using the standard pulse sequence. HMBC (heteronuclear multiple-bond correlation) spectra were recorded with a relaxation delay of 1.5 s. Experimental data were processed on a Pentium IV PC using MestReNOVA 5.3 software (Mestrelab Research SL, CA).

2.10. Statistical analysis

Data were presented as mean ± SEM. Statistical significance was defined as $p < 0.05$ after analyzing with Student's t-test.

3. Results

3.1. Characterization of PSs from cultured mycelia of A. cinnamomea

The crude PS, B85PS (40 mg), was fractionated into Fr-I (28–32), -II (33–36), -III (37–40), -IV (41–50), and -V (51–56) on a Fractogel BioSec 80 cm × 1.5 cm column (Merck) as described in Section 2.2 (Fig. 1A). Fraction III (B85PS-III) demonstrated the most potent angiogenic inhibition with an IC_{50} of 7.07 μg/ml, and it was further subjected to SEC to give three subfractions (III-1–3, 1.7, 2.7 and 0.2 mg, respectively). B85PS-III-1 was eluted from a series connection of one G3000 and one G4000 column on HPLC (Fig. 1B). Its molecular mass was estimated to be 4.17×10^2 kDa by SEC as aforementioned. Hydrolysates of B85PS-III-1 contained galactose, fucose and mannose in a ratio of 13:4:2 (Table 1).

3.2. In vitro angiogenesis assay

Fractionated PSs from *A. cinnamomea* B85 showed differential inhibition of *in vitro* Matrigel tube formation (Fig. 2), a standard assay for angiogenesis. After calculating the percentage of the tube formation area by angiogenesis software, B85PS showed inhibition of Matrigel tube formation with an IC_{50} of 19.1 μg/ml. However, after fractionation, subfractions I, II, III, IV, and V showed discriminative inhibitory effect on Matrigel tube formation, with IC_{50} values of 7.44, 16.41, 7.07, 7.98, and 16.33 μg/ml, respectively. Three parameters including the total percent of tube formation area, tube length, and branch numbers for different concentration treatments of the B85 fractionated PSs (data not shown). All fractionated B85 PSs dose-dependently inhibited Matrigel tube formation and these calculated parameters.

Table 1
Sugar composition for three polysaccharide subfractions of B85PS-III from *A. cinnamomea*.

	Neutral sugars (μmol/g fractionated PS)[a]		
	B85PS-III-1	B85PS-III-2	B85PS-III-3
Myo-inositol	18.76 ± 2.82	17.54 ± 1.13	2.14 ± 0.01
Sorbitol	19.03 ± 15.60	17.18 ± 3.94	1.58 ± 0.02
Fucose	72.89 ± 18.32	32.05 ± 7.35	0.33 ± 0.05
Galactosamine	8.23 ± 1.62	12.09 ± 6.09	0.00
Glucosamine	8.55 ± 1.36	0.00	0.39 ± 0.2
Galactose	237.18 ± 16.32	77.4 ± 6.52	2.7 ± 0.20
Glucose	17.49 ± 3.64	48.27 ± 2.14	6.17 ± 0.04
Mannose	31.04 ± 6.84	20.87 ± 1.39	3.31 ± 0.28
Fructose	12.62 ± 8.06	0.00	0.00

[a] Values represent the average of duplicate assays ± S.E.

3.3. Cell migration and in vivo angiogenesis assay

Cell migration is involved in angiogenesis. Therefore, the EC migration ability of B85PS and fractionated PSs (B85PS-I–V) from *A. cinnamomea* B85 were tested using a wound healing assay (Fig. 3). Crude B85 and B85PS I–V dose-dependently inhibited VEGF-induced EC migration.

3.4. Evaluation of angiogenic-related protein expressions

ECs were pretreated with B85PS, B85PS-III, or B85PS-V for 1 h following VEGF incubation for 24 h. Then cell lysates were collected to evaluate the expression of VEGFR activity and Ang-2 expression using identical antibodies against these proteins (Fig. 4). B85 crude PSs, B85PS-III and B85PS-V, dose-dependently inhibited phosphorylated VEGFR and Ang-2 expressions. These results indicated that B85 fractionated PSs might participate in attenuating angiogenesis processes.

3.5. 1D and 2D NMR

The completely assigned spectra of the PS, given in Table 2, were derived from ^1H, ^{13}C, DQF-COSY, TOCSY, NOESY, HSQC and HMBC NMR spectra.

3.5.1. General observations

The ^1H NMR spectrum of B85PS-III-1 showed four anomeric protons at δ_H 5.08, 5.06, 5.02, and 4.98. The sugar residues were designated as follows: δ 4.98 for residue A, δ 5.02 for residue B, δ_H 5.06 for residues C, E and F, and δ_H 5.08 for residue D (Table 2), according to their H-1 chemical shift values in ascending order. The signals at δ_H 4.98, 5.02, and 5.06 were appeared as singlets ($^3J_{1,2} < 3$ Hz), indicating that the sugars were with α-anomeric configuration. The ^{13}C NMR spectrum (Fig. 5) showed one major signal for three anomeric carbons at δ_C 99.4, 99.3, and 99.2, two substituted hydroxymethylene carbon at δ_C 67.9 and 68.2 (both C-6 glycosylated), and one CH_3–C group (C-6 of Fuc) at δ_C 17.2. No signal for the unsubstituted hydroxymethylene protons in the region of δ_C 57–63 was observed, suggesting that all C-6 s were glycosylated.

The proton and carbon NMR data of B85PS-III-1 were completely assigned (Table 2) according to 1D (^1H, ^{13}C and DEPT-135) and 2D (NOESY, DQF-COSY, TOCSY, HSQC and HMBC) NMR spectra. The following sections described the six types of sugar residues (residues A–F) observed in the HSQC spectrum (Fig. 6A).

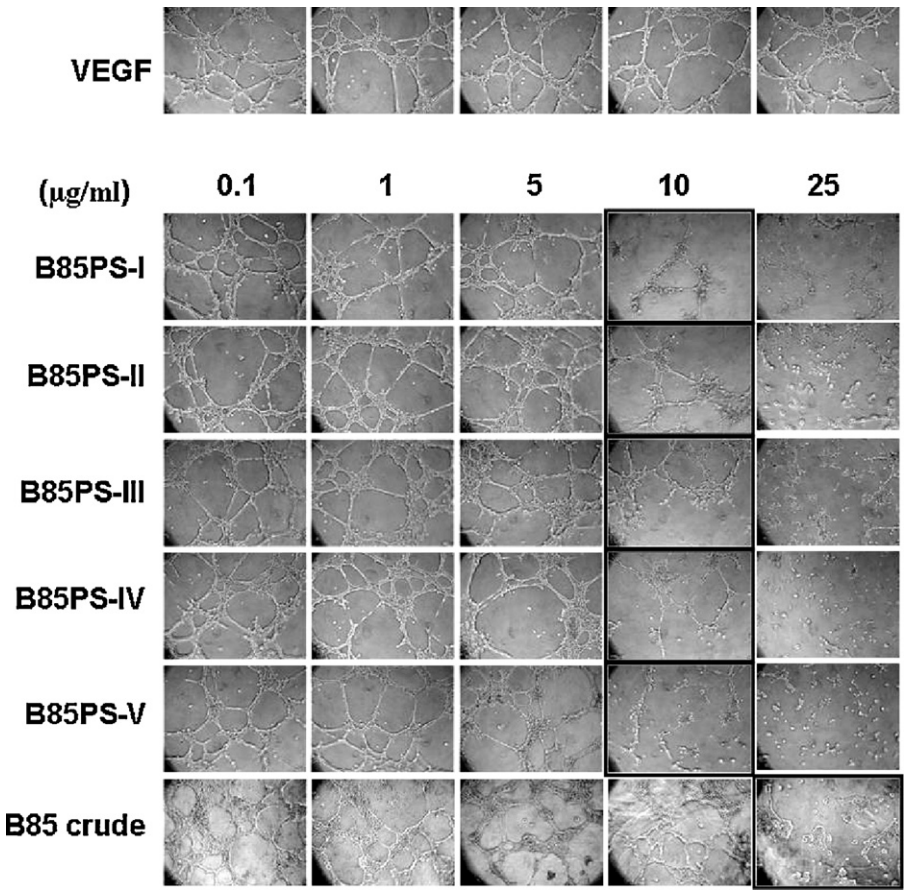

Fig. 2. Dose-dependent inhibition of crude and fractionated polysaccharides (PSs) from *A. cinnamomea* B85 on Matrigel tube formation in endothelial cells (ECs). ECs were seeded onto Matrigel and cultured for 24 h under vascular endothelial growth factor (VEGF) supplementation with or without pretreatment of serial concentrations of the test components. Capillary tube formation on Matrigel was visualized with an inverted ZEISS microscope at a magnification of 10×. The black frame indicated the estimated inhibition concentration of each component.

3.5.2. Residue A assignment

The complete proton and carbon chemical shifts (Table 2) of the spin system beginning from the peak at δ_H 4.98 was obtained from the TOCSY, NOESY, and HMBC spectra. The TOCSY spectrum showed stepwise connectivities for the H-1 signal at δ_H 4.98 to H-2 at δ_H 3.84, H-3 at δ_H 3.89, and H-4 at δ_H 4.02. The HMBC spectrum (Fig. 6B) demonstrated correlations between the H-5 at δ_H 4.21 and the C-6 signal at δ_C 67.9, between the H-3 at δ_H 3.89 and the C-2 signal at δ_C 69.7, and between the H-2 at δ_H 3.84 and the C-3 signal at δ_C 70.9. In addition, the C-3 and C-5 signals (at δ_C 70.9 and 70.2, respectively) demonstrated $^3J_{C,H}$ correlations to the H-1 at δ_H 4.98, and the C-4 signal at δ_C 70.9 showed correlations to δ_H 3.84 (H-2) and δ_H 3.89 (H-3). The downfield-shifted ^{1}H (δ_H 3.93 and 3.68) and ^{13}C (δ_C 67.9) chemical shifts prompted the signals for the 6-*O*-substituted methylene of a pyranoside. The monosaccharide analysis (Table 1) implied that the residue A was galactose, the major monosaccharide. These evidences suggested that residue A was a 6-substituted α-D-galactopyranoside.

3.5.3. Residue B assignment

The spin system of residue B, which was starting from the H-1 signal at δ_H 5.02, was completely assigned (Table 2). Similar to residue A, the downfield-shifted methylene signal at δ_C 67.9 in DEPT-135 indicated a C-6 glycosidic linkage. The ^{13}C and ^{1}H NMR

Table 2
^{1}H and ^{13}C chemical shift data of the monosaccharides constituting B85PS-III-1 from *A. cinnamomea*.

Residue	^{1}H/^{13}C δ (ppm)					
	1	2	3	4	5	6
A	4.98	3.84	3.91	4.02	4.21	3.93 (a), 3.68 (b)
α-D-Gal$_{4.98}$	99.2	69.7	70.9	70.9	70.2	67.9
B	5.02	3.85	3.89	3.68	4.26	3.93 (a), 3.68 (b)
α-D-Gal$_{5.02}$	99.4	69.6	70.9	80.0	70.1	67.9
C	5.06	3.85	3.90	4.08	4.24	3.93 (a), 3.68 (b)
α-D-Gal$_{5.06}$	99.3	79.2	70.9	70.9	70.2	67.9
D	5.08	3.58	3.83	4.16	4.09	1.25
α-L-Fuc$_{5.08}$	99.3	68.5	69.7	70.6	68.9	17.2
E	5.06	3.64	3.89	4.18	3.97	1.24
α-L-Fuc$_{5.06}$	99.3	68.6	69.8	70.6	68.5	17.2
F	5.06	4.02	3.67	3.64	3.89	3.90 (a), 3.73 (b)
α-D-Man$_{5.06}$	102.7	71.3	70.7	67.8	74.1	68.2

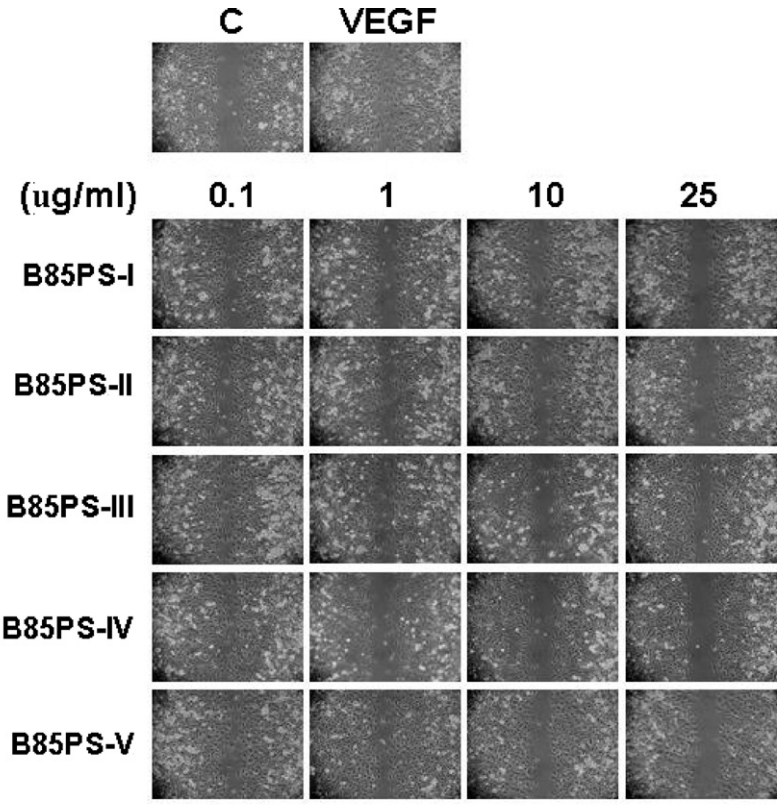

	0.1	1	10	20
B85-PS-I	111.2±18.3	79.2±8.7	65.8±7.3	56.7±9.5
B85-PS-II	103.8±10.8	92.6±9.8	109±8.5	54.7±11.5
B85-PS-III	100.6±12.3	90.1±10.4	85.6±8.7	66.8±9.3
B85-PS-IV	98.4±9.8	56.1±8.3	80.5±9.3	50.7±7.1
B85-PS-V	95.7±12.4	100.4±11.3	78.9±9.7	41.5±6.6

Fig. 3. Migration activity of crude and fractionated polysaccharides (PSs) from *A. cinnamomea* B85 on endothelial cells (ECs) using a wound healing assay. (A) An endothelial migration assay was performed by scraping ECs from the middle of the coverslip, leaving a 500-μm area devoid of cells. ECs were washed and cultured for 4 h with or without vascular endothelial growth factor (VEGF) and pretreatment with serial concentrations of crude or fractionated PSs from *A. cinnamomea* B85. The migration of ECs was visualized with an inverted Nikon/TMS microscope at a magnification of 10×. Migrated cells were calculated and represented as mean ± S.E. in three independent experiments.

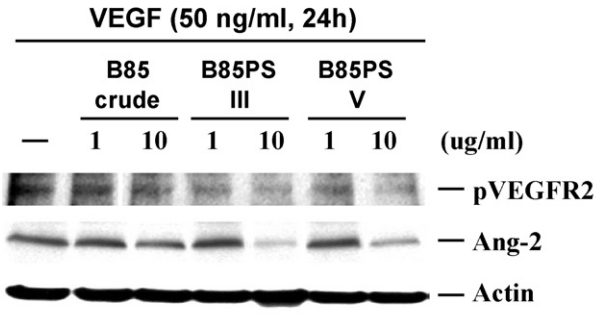

	VEGF	Crude-1	Crude-10	III-1	III-10	V-1	V-10
pVEGFR2	100	88.8±10.3	78.2±4.7	56.3±9.6	41.3±7.1	63.8±8.5	45.1±8.3
Ang-2	100	52.6±9.4	38.5±8.3	54.7±10.5	8.9±13.1	58.3±9.6	20.8±7.5

Fig. 4. Effects of crude and fractionated polysaccharides (PSs) from *A. cinnamomea* B85 on vascular endothelial growth factor receptor (VEGFR) tyrosine phosphorylation and angiopoietin (Ang)-2 protein expressions. Endothelial cells (ECs) were treated with crude and fractionated polysaccharides (PSs) (III and V) from *A. cinnamomea* B85 at different concentrations for 24 h. After treatment, cells are lysed and examined for the protein expressions of VEGFR tyrosine phosphorylation (pVEGFR) and Ang-2 by an immunoblot assay. Actin was detected to indicate equal amounts of protein in each lane. Data were representative of three independent experiments with similar results. Density of each band was calculated with densitometer and normalized with actin group and calculated as percentage of VEGF group (as 100%).

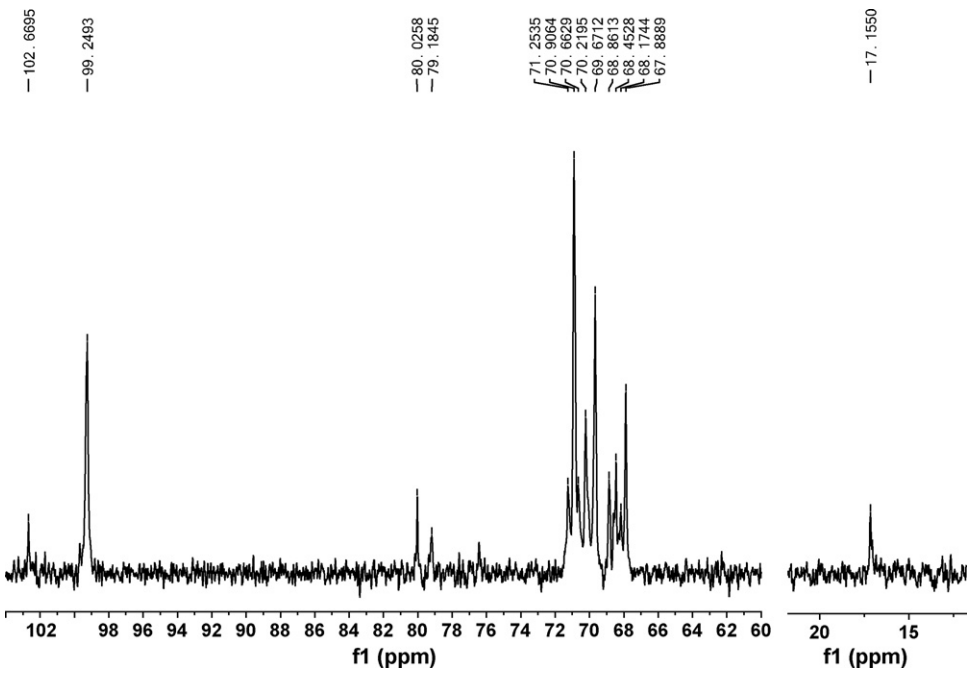

Fig. 5. ^{13}C nuclear magnetic resonance spectrum (150 MHz) of B85PS-III-1 from *A. cinnamomea* in D_2O at 25 °C. Chemical shifts were shown in δ ppm.

data of residue B were fully specified from the C–H pairs (Table 2) of the HSQC spectrum (Fig. 6A). One ^3J and one ^2J correlations in the HMBC spectrum, δ_H 5.02 (H-1)/δ_C 70.9 (C-3) and δ_H 3.85 (H-2)/δ_C 70.9 (C-3), respectively, were observed. In addition, the HMBC and HSQC spectra showed a correlation between the downfield-shifted ^{13}C signal at δ_C 79.2 (C-4) and the ^1H at δ_H 3.68 (H-4), and the TOCSY indicated a correlation between H-4 at δ_H 3.68 and H-6a at δ_H 3.93. On the basis of the aforementioned evidence, the structure of residue B was elucidated to be a α-D-galactopyranoside with 1,4,6-tri-*O*-substitutions.

3.5.4. Residue C assignment

The ^1H and ^{13}C NMR data of residue C showed a signal pattern similar to that of residue B, a typical 6-*O*-substituted galactopyranoside but with a C-2 substitution, instead of a C-4 substitution in residue B. Using the aforementioned approaches, the complete ^1H and ^{13}C chemical shifts for residue C (Table 2) were readily assigned from the HSQC spectrum (Fig. 6A). The HMBC spectrum showed correlations of δ_H 5.06 (H-1) with δ_C 79.2 (C-2), and of δ_H 3.85 (H-2) with δ_C 70.9 (C-3 and C-4). Similar to residues A and B, the DEPT-135 spectrum indicated a C-6 glycosidic linkage. The TOCSY spectrum demonstrated correlations of H-1 at δ_H 5.06 with H-2 at δ_H 3.85 and H-4 at δ_H 4.08. As a result, residue C was assigned as a 1,2,6-tri-*O*-substituted α-D-galactopyranoside.

3.5.5. Residues D and E assignment

The ^1H and ^{13}C NMR data of residues D and E (Table 2), which were started from the anomeric proton signals at δ_H 5.08 (D H-1) and δ_H 5.06 (E H-1), were assigned by similar methods. For residue D, stepwise connectivities were observed in the TOCSY spectrum, including the signals from H-1 at δ_H 5.08 to H-2 at δ_H 3.58, H-3 at δ_H 3.83, and H-5 at δ_H 4.09, from H-6 at δ_H 1.25 to H-5 at δ_H 4.09 and H-4 at δ_H 4.16, and from H-2 at δ_H 3.58 to H-5 at δ_H 4.09 and H-3 at δ_H 3.83. Signals for H-2 and H-5 were confirmed by cross peaks in the HMBC spectrum, including H-6 at δ_H 1.25 to C-5 at δ_C 68.9, and H-1 at δ_H 5.08 to C-2 at δ_C 68.5. The DQF-COSY spectrum demonstrated a correlation between δ_H 4.16 (H-4) and δ_H 1.25 (H-6), and between δ_H 3.83 (H-3) and δ_H 1.25 (H-2). Likewise, the TOCSY spectrum of residue E showed distinctive connectivities from H-6 at δ_H 1.24 to H-5 at δ_H 3.97 and H-4 at δ_H 4.18, and from H-2 at δ_H 3.64 to H-3 at δ_H 3.73 and H-4 at δ_H 4.18. In addition, the HMBC spectrum confirmed the signals for H-2 (δ_H 3.64) and H-5 (δ_H 3.97). The H-6 (δ_H 1.25/1.24)/C-6 (δ_C 17.2) suggested a 6-deoxy-pyranoside. The monosaccharide analysis (Table 1) showed the only deoxy-monosaccharide was L-fuc. Thus, these two residues were identified as two α-L-fucopyranosides.

3.5.6. Residue F assignment

The cross peaks for residue F were observed in the HSQC spectrum, including δ 5.06/102.7 (H-1/C-1), δ 4.02/71.3 (H-2/C-2), δ 3.67/70.7 (H-3/C-3), δ 3.64/67.8 (H-4/C-4), and δ 3.90,3.73/68.2 (H-6 s/C-6) (Fig. 3A). No correlation was observed in the HMBC spectrum because of the limited material. However, the TOCSY spectrum showed connectivities from H-2 (δ_H 4.02) to H-3 (δ_H 3.67), H-4 (δ_H 3.64), H-5 (δ_H 3.89) and H-6 s (δ_H 3.73 and 3.90), and from H-3 (δ_H 3.67) to H-5 (δ_H 3.89) and H-6a (δ_H 3.90). The correlations from H-2 (δ_H 4.02) to H-3 (δ_H 3.67) and H-5 (δ_H 3.89) in the NOESY spectrum confirmed the assignment. The carbon chemical shifts of C-1 (δ_C 102.7), C-5 (δ_C 74.1) and C-6 (δ_C 68.2) at low field and the result of monosaccharide analysis (Table 1) suggested that residue F was a α-D-Man residue (Cho, Koshino, Yu, & Yoo, 1998), specifically a 1,6-di-*O*-substituted α-D-mannopyranoside.

3.5.7. Assignment of the residue linkages

The inter-residue connectivities were observed in the NOESY, TOCSY and HMBC spectra of B58PS-III-1. The D(1 → 4)B linkage was identified by the inter-residue correlations between D H-1 and B H-4 observed in the TOCSY spectrum, and between D H-1 at δ_H 5.08 and B C-4 at δ_C 79.2 in the HMBC spectrum. The TOCSY and NOESY spectra revealed the correlation between E H-1 at δ_H 5.08 and C H-2 at δ_H 3.85, indicative of an E(1 → 2)C linkage.

Since the ratio of Gal:Fuc:Man was determined as 13:4:2 in monosaccharide analysis, integration of the anomeric signals for residue A (δ_H 4.98), residue B (δ_H 5.02), residues C/E/F (δ_H 5.06)

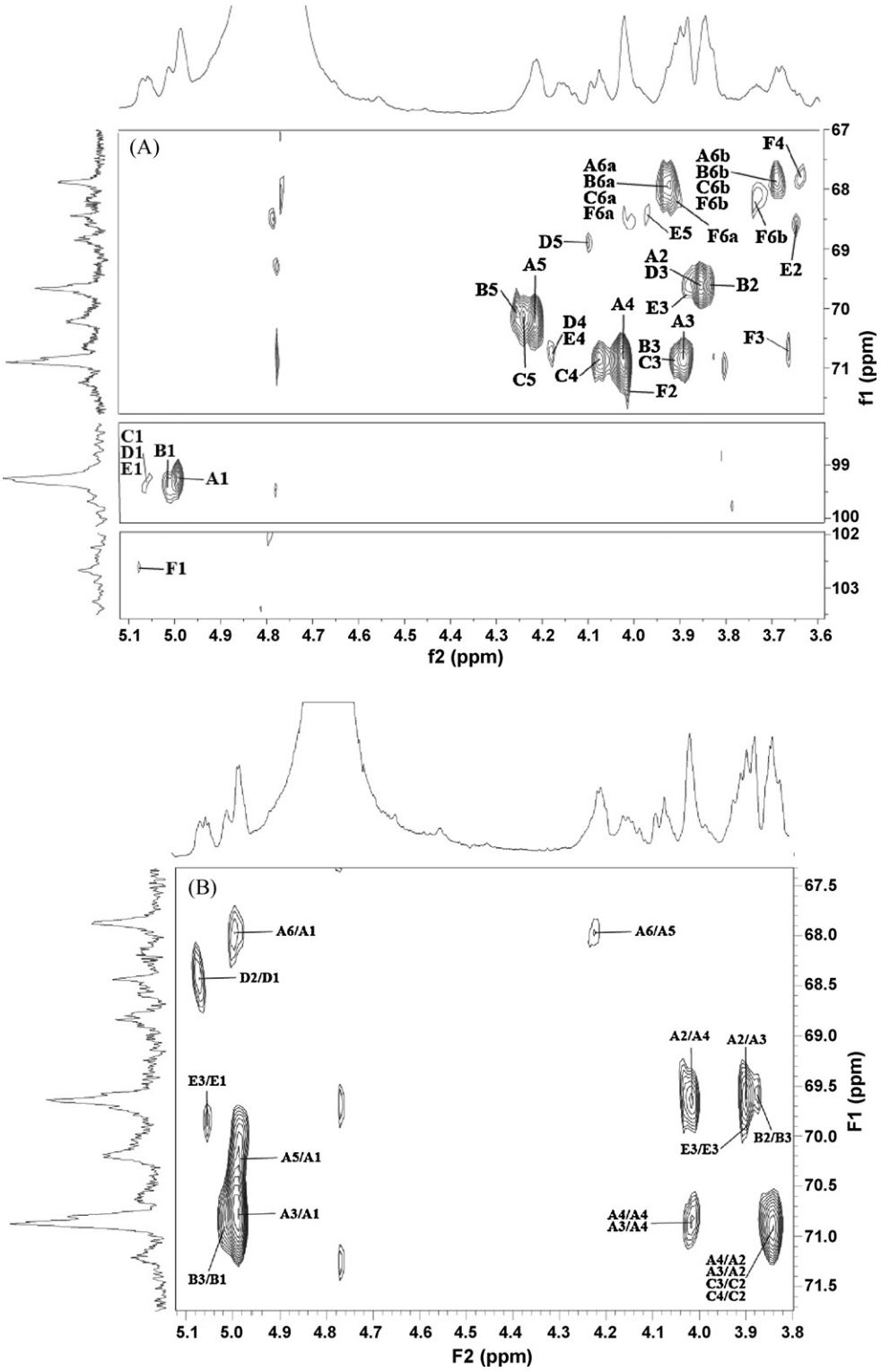

Fig. 6. 2D HSQC (A) and HMBC (B) nuclear magnetic resonance spectra of B85PS-III-1 from *A. cinnamomea* in D_2O at 25 °C.

and residue D (δ_H 5.08) in the ^1H spectrum gave a ratio of ca. 9:3:4:3, suggesting that the ratio of residues A:B:C was 9:3:1, and thus residues (E + F):D was considered to be 1:1. Accordingly, the ratio of residues A:B:C:D:E:F was further resolved as 9:3:1:3:1:2. These results suggested that B85PS-III-1 had a back bone of (1 → 6)-linked D-galactopyranosyl residues and approximately every other third of these were substituted at the 4-*O* and 2-*O* positions (at a ratio of 3:1) by an α-L-fucosyl unit made up of partial 2-*O*- and 4-*O*-α-L-fucosylated 1,6-α-D-galactopyranosyl repeats. Because the α-D-mannosyl residue also appeared as a non-terminal (1 → 6)-linked unit, it should be existed between two residue A units. Therefore, a tentative partial nonadecasaccharide repeating unit for B85PS-III-1, as shown below, was proposed.

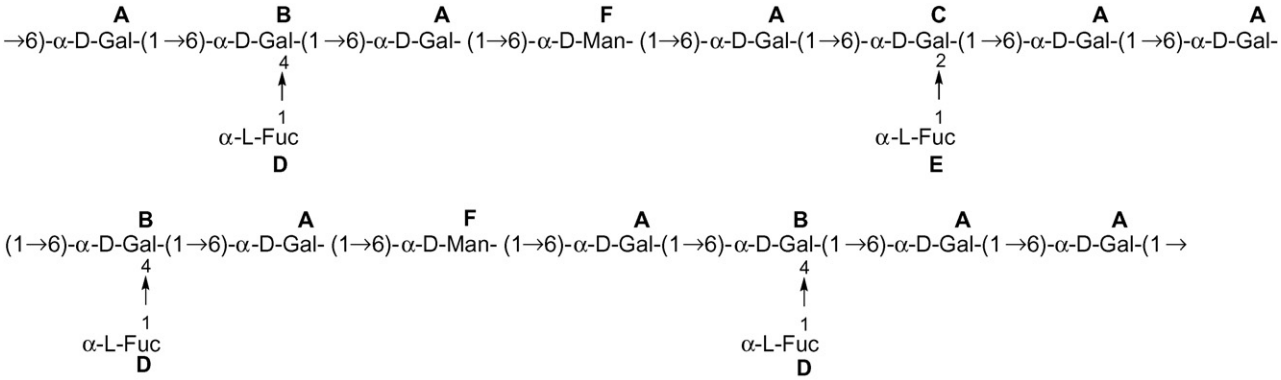

Thirteen D-galactopyranosyl residues (residue A × 9; residue B × 3; residue C × 1) and two D-mannopyranosyl residues between two A residues were present as the main skeleton linked at the 6-*O* position, as residues with interchangeable substitutions at the 4-*O* (residue D) and 2-O (residue E) positions with a ratio of 3:1 in the repeat unit.

4. Discussion

In this article, we reported the isolation, identification, and antiangiogenic activities of a partial 2-*O*- and 4-*O*-α-L-fucosylated 1,6-α-D-mannogalactan B85PS-III-1 from fermented mycelia of *A. cinnamomea*. For the species studied in this report, no structural elucidation of the PS component had previously been reported to our knowledge. The skeleton of the 1,6-α-D-galactopyranosyl moiety was also found in a number of fungi, such as *Coprinus comatus* (Fan et al., 2006), *Laetiporus sulphureus* (Bull.: Fr.) Murr. (Alquini, Carbonero, Rosado, Cosentino, & Iacomini, 2004), and *Fomitella fraxinea* (Imaz.) (Cho et al., 1998). Among the PSs in the fungal cell wall, glucans are the most widely-distributed carbohydrate, often with β-1,3-linkages. In addition, heterogalactans, especially with a fucose terminal, were reported in basidiomycetes (Cho et al., 1998; Alquini et al., 2004; Fan et al., 2006).

Different PS subfractions in this study exhibited differential inhibition of angiogenesis-related processes, including EC tube formation and cell migration. In particular, the B85PS-III subfraction consists of a novel water-soluble 1,6-α-D-mannogalactan with a partial 2-*O*- and 4-*O*-α-L-fucosyl terminals. We isolated natural molecules with related structure (as B85PS-III-1) from *Poria cocos* (Lu et al., 2010) and gave a 1,6-branched 1,3-α-D-galactan. The structure differed from B85PS-III-1 in the α-1,3 main skeleton and a high ratio of α-1,6 branches. We tested its antiangiogenic activity. PC-II exhibited no inhibitory effect on EC tube formation compared to VEGF-treated control cells (data not shown). It was reported that the galactose and fucose contents in PSs are required for inhibition properties against angiogenesis (Holle et al., 2004; Matsubara et al., 2005). In the structural feature of B85PS-III-1, galactose and fucose was the major sugar components. The biological activity of B85PS-III-1 could be due to galactose- or fucose-containing linkage in structure which may be important for its activity.

Ang-2 plays an important role in vascular remodeling. Serum Ang-2 was reported to be a clinical marker for lung cancer (Park et al., 2007). Systemic anti-Ang-2 therapy inhibiting tumor growth and angiogenesis in preclinical models was reported (Cao et al., 2007). Ang-2 can initiate angiogenic signal following locally opening up the vessel structure and proceeding protease degradation of the basement membrane around the endothelium. In consequence increase accessibility to that endothelium by angiogenesis inducers such as VEGF, thereby increasing capillary sprouting and new blood vessels formation (Hanahan, 1997). In this study, B85PS-III and its subfractions dose-dependently inhibited VEGFR phosphorylation, which is required for VEGFR activation. Furthermore, they also inhibited Ang-2 protein expression. These results indicate that the antiangiogenic inhibition property of B85PS-III may occur through suppression of VEGFR activation and Ang-2 expression.

5. Conclusion

In conclusion, the antiangiogenic effects and a proposed repeating unit of a novel water-soluble 1,6-α-D-mannogalactan with partial 2- and 4-α-L-fucosyl terminals from cultured *A. cinnamomea* were reported.

Acknowledgements

We thank Mr. Dan Chamberlin for linguistic revision of the manuscript. This work was supported in part by grants (NRICM97-DBCM-08) to JJC, (NRICM-98-DHM-03) to MKL, and (NRICM-98-DMC-08) to CCC from the National Research Institute of Chinese Medicine, Taipei, Taiwan.

References

Alquini, G., Carbonero, E. R., Rosado, F. R., Cosentino, C., & Iacomini, M. (2004). Polysaccharides from the fruit bodies of the basidiomycete *Laetiporus sulphureus* (Bull.: Fr.) Murr. *FEMS Microbiology Letters*, *230*, 47–52.

Boehm, T., Folkman, J., Browder, T., & O'Reilly, M. S. (1997). Antiangiogenic therapy of experimental cancer does not induce acquired drug resistance. *Nature*, *390*, 404–407.

Cao, Y., Sonveaux, P., Liu, S., Zhao, Y., Mi, J., Clary, B. M., et al. (2007). Systemic overexpression of angiopoietin-2 promotes tumor microvessel regression and inhibits angiogenesis and tumor growth. *Cancer Research*, *67*, 3835–3844.

Chang, C. Y., Huang, Z. N., Yu, H. H., Chang, L. H., Li, S. L., Chen, Y. P., et al. (2008). The adjuvant effects of *Antrodia camphorata* extracts combined with anti-tumor agents on multidrug resistant human hepatoma cells. *Journal of Ethnopharmacology*, *118*, 387–395.

Chen, Y. J., Cheng, P. C., Lin, C. N., Liao, H. F., Chen, Y. Y., Chen, C. C., et al. (2008). Polysaccharides from *Antrodia camphorata* mycelia extracts possess immunomodulatory activity and inhibits infection of *Schistosoma mansoni*. *International Immunopharmacology*, *8*, 458–467.

Cheng, J. J., Yang, C. J., Cheng, C. H., Wang, Y. T., Huang, N. K., & Lu, M. K. (2005). Characterization and functional study of *Antrodia camphorata* lipopolysaccharide. *Journal of Agricultural and Food Chemistry*, *53*, 469–474.

Cheng, J. J., Huang, N. K., Chang, T. T., Wang, D. L., & Lu, M. K. (2005). Study for antiangiogenic activities of polysaccharides isolated from *Antrodia cinnamomea* in endothelial cells. *Life Sciences*, *76*, 3029–3042.

Cheng, J. J., Lin, C. Y., Lur, H. S., Chen, H. P., & Lu, M. K. (2008). Properties and biological functions of polysaccharides and ethanolic extracts isolated from medicinal fungus, *Fomitopsis pinicola*. *Process Biochemistry (Barking, London, England)*, *43*, 829–834.

Cheng, P. C., Hsu, C. Y., Chen, C. C., & Lee, K. M. (2008). *In vivo* immunomodulatory effects of *Antrodia camphorata* polysaccharides in a T1/T2 doubly transgenic mouse model for inhibiting infection of *Schistosoma mansoni*. *Toxicology and Applied Pharmacology*, *227*, 291–298.

Cherng, I. H., Wu, D. P., & Chiang, H. C. (1996). Triterpenoids from *Antrodia cinnamomea*. *Phytochemistry*, *41*, 263–267.

Chiang, H., Wu, D., Cherng, I., & Ueng, C. (1995). A sesquiterpene lactone, phenyl and biphenyl compounds from *Antrodia cinnamomea*. *Phytochemistry*, *39*, 613–616.

Cho, S. K., Koshino, H., Yu, S. H., & Yoo, I. D. (1998). A mannofucogalactan, fomitellan A, with mitogenic effect from fruit bodies of *Fomitella fraxinea* (Imaz.). *Carbohydrate Polymers*, *37*, 13–18.

Fan, J. M., Zhang, J. S., Tang, Q. J., Liu, Y. F., Zhang, A. Q., & Pan, Y. J. (2006). Structural elucidation of a neutral fucogalactan from the mycelium of *Coprinus comatus*. *Carbohydrate Research*, *341*, 1130–1134.

Hanahan, D. (1997). Signaling vascular morphogenesis and maintenance. *Science*, *277*, 48–50.

Holle, L., Song, W., Hicks, L., Holle, E., Holmes, L., Wei, Y., et al. (2004). In vitro targeted killing of human endothelial cells by co-incubation of human serum and NGR peptide conjugated human albumin protein bearing alpha (1–3) galactose epitopes. *Oncology Reports*, *11*, 613–616.

Hsu, Y. L., Kuo, Y. C., Kuo, P. L., Ng, L. T., Kuo, Y. H., & Lin, C. C. (2005). Apoptotic effects of extract from *Antrodia camphorata* fruiting bodies in human hepatocellular carcinoma cell lines. *Cancer Letters*, *221*, 77–89.

Huang, S. J., & Mau, J. L. (2007). Antioxidant properties of methanolic extracts from *Antrodia camphorata* with various doses of γ-irradiation. *Food Chemistry*, *105*, 1702–1710.

Karamysheva, A. F. (2008). Mechanisms of angiogenesis. *Biochemistry (Moscow)*, *73*, 751–762.

Lee, I. H., Huang, R. L., Chen, C. T., Chen, H. C., Hsu, W. C., & Lu, M. K. (2002). Antrodia camphorata polysaccharide exhibits anti-hepatitis B virus effects. *FEMS Microbiology Letters*, *209*, 63–67.

Liu, J. J., Huang, T. S., Hsu, M. L., Chen, C. C., Lin, W. S., Lu, F. J., et al. (2004). Antitumor effects of the partially purified polysaccharides from *Antrodia camphorata* and the mechanism of its action. *Toxicology and Applied Pharmacology*, *201*, 186–193.

Lu, M. C., Hwang, S. L., Chang, F. R., Chen, Y. H., Chang, T. T., Hung, C. S., et al. (2009). Immunostimulatory effect of *Antrodia camphorata* extract on functional maturation of dendritic cells. *Food Chemistry*, *113*, 1049–1057.

Lu, M. K., Cheng, J. J., Lai, W. L., Lin, Y. J., & Huang, N. K. (2008). Fermented *Antrodia cinnamomea* extract prevents rat PC12 cells from serum deprivation-induced apoptosis: The role of the MAPK family. *Journal of Agricultural and Food Chemistry*, *56*, 865–874.

Lu, M. K., Cheng, J. J., Lin, C. Y., & Chang, C. C. (2010). Purification, structural elucidation, and anti-inflammatory effect of a water-soluble 1,6-branched 1,3-α-D-galactan from cultured mycelia of *Poria cocos*. *Food Chemistry*, *118*, 349–356.

Mandriota, S. J., & Pepper, M. S. (1998). Regulation of angiopoietin-2 mRNA levels in bovine microvascular endothelial cells by cytokines and hypoxia. *Circulation Research*, *83*, 852–859.

Matsubara, K., Xue, C., Zhao, X., Mori, M., Sugawara, T., & Hirata, T. (2005). Effects of middle molecular weight fucoidans on in vitro and ex vivo angiogenesis of endothelial cells. *International Journal of Molecular Medicine*, *15*, 695–699.

Park, J. H., Park, K. J., Kim, Y. S., Sheen, S. S., Lee, K. S., Lee, H. N., et al. (2007). Serum angiopoietin-2 as a clinical marker for lung cancer. *Chest*, *132*, 200–206.

Shen, Y. C., Chou, C. J., Wang, Y. H., Chen, C. F., Chou, Y. C., & Lu, M. K. (2004). Anti-inflammatory activity of the extracts from mycelia of *Antrodia camphorata* cultured with water-soluble fraction from five different *Cinnamomum* genera. *FEMS Microbiology Letters*, *231*, 137–143.

Wu, D. P., & Chiang, H. C. (1995). Constituents of *Antrodia cinnamomea*. *Journal of the Chinese Chemical Society*, *42*, 797–800.

Wu, S. H., Ryvarden, L., & Chang, T. T. (1997). Antrodia camphorata ("niu-chang-chih"), new combination of a medicinal fungus in Taiwan. *Botanical Bulletin of Academia Sinica (Taiwan)*, *38*, 273–275.

Yang, C. M., Zhou, Y. J., Wang, R. J., & Hu, M. L. (2009). Anti-angiogenic effects and mechanisms of polysaccharides from *Antrodia cinnamomea* with different molecular weights. *Journal of Ethnopharmacology*, *123*, 407–412.